CDF/PUB/HEAVYFLAVOR/PUBLIC/1306
October 12, 1990
Fermilab-CONF-90/255-E
December 10, 1990

B-PHYSICS at CDF

A.R.Baden
University of Maryland

F. Abe,[8] D. Amidei,[4] G. Apollinari,[11] M. Atac,[4] P. Auchincloss,[14]
A. R. Baden,[6] A. Bamberger,[19] A. Barbaro-Galtieri,[9] V. E. Barnes,[12]
F. Bedeschi,[11] S. Behrends,[2] S. Belforte,[11] G. Bellettini,[11] J. Bellinger,[18]
J. Bensinger,[2] A. Beretvas,[4] J. P. Berge,[4] S. Bertolucci,[5] S. Bhadra,[7]
M. Binkley,[4] R. Blair,[1] C. Blocker,[2] A. W. Booth,[4] G. Brandenburg,[6]
D. Brown,[6] E. Buckley,[14] A. Byon,[12] K. L. Byrum,[18] C. Campagnari,[3]
M. Campbell,[3] R. Carey,[6] W. Carithers,[9] D. Carlsmith,[18] J. T. Carroll,[4]
R. Cashmore,[19] F. Cervelli,[11] K. Chadwick,[4] G. Chiarelli,[5]
W. Chinowsky,[9] S. Cihangir,[4] A. G. Clark,[4] D. Connor,[10] M. Contreras,[2]
J. Cooper,[4] M. Cordelli,[5] D. Crane,[4] M. Curatolo,[5] C. Day,[4]
S. Dell'Agnello,[11] M. Dell'Orso,[11] L. Demortier,[2] P. F. Derwent,[3]
T. Devlin,[14] D. DiBitonto,[15] R. B. Drucker,[9] J. E. Elias,[4] R. Ely,[9]
S. Errede,[7] B. Esposito,[5] B. Flaugher,[14] G. W. Foster,[4] M. Franklin,[6]
J. Freeman,[4] H. Frisch,[3] Y. Fukui,[8] Y. Funayama,[16] A. F. Garfinkel,[12]
A. Gauthier,[7] S. Geer,[6] P. Giannetti,[11] N. Giokaris,[13] P. Giromini,[5]
L. Gladney,[10] M. Gold,[9] K. Goulianos,[13] H. Grassmann,[11]
C. Grosso-Pilcher,[3] C. Haber,[9] S. R. Hahn,[4] R. Handler,[18] K. Hara,[16]
R. M. Harris,[9] J. Hauser,[3] T. Hessing,[15] R. Hollebeek,[10] L. Holloway,[7]
P. Hu,[14] B. Hubbard,[9] B. T. Huffman,[12] R. Hughes,[10] P. Hurst,[7]
J. Huth,[4] M. Incagli,[11] T. Ino,[16] H. Iso,[16] H. Jensen,[4] C. P. Jessop,[6]
R. P. Johnson,[4] U. Joshi,[4] R. W. Kadel,[4] T. Kamon,[15] S. Kanda,[16]
D. A. Kardelis,[7] I. Karliner,[7] E. Kearns,[6] R. Kephart,[4] P. Kesten,[2]
R. M. Keup,[7] H. Keutelian,[7] S. Kim,[16] L. Kirsch,[2] K. Kondo,[16]
S. E. Kuhlmann,[1] E. Kuns,[14] A. T. Laasanen,[12] J. I. Lamoureux,[18]
W. Li,[1] T. M. Liss,[7] N. Lockyer,[10] C. B. Luchini,[7] P. Maas,[4]
M. Mangano[11] J. P. Marriner,[4] R. Markeloff,[18] L. A. Markosky,[18]
R. Mattingly,[2] P. McIntyre,[15] A. Menzione,[11] T. Meyer,[15] S. Mikamo,[8]
M. Miller,[3] T. Mimashi,[16] S. Miscetti,[5] M. Mishina,[8] S. Miyashita,[16]
Y. Morita,[16] S. Moulding,[2] A. Mukherjee,[4] L. F. Nakae,[2] I. Nakano,[16]
C. Nelson,[4] C. Newman-Holmes,[4] J. S. T. Ng,[6] M. Ninomiya,[16]
L. Nodulman,[1] S. Ogawa,[16] R. Paoletti,[11] A. Para,[4] E. Pare,[6]
J. Patrick,[4] T. J. Phillips,[6] R. Plunkett,[4] L. Pondrom,[18] J. Proudfoot,[1]

Pub. Proceedings SLAC Summer School Topical Conference on Gauge Bosons and Heavy Quarks, SLAC, Stanford, CA, July 25-27, 1990.

G. Punzi,[11] D. Quarrie,[4] K. Ragan,[10] G. Redlinger,[3] J. Rhoades,[18]
M. Roach,[17] F. Rimondi,[19] L. Ristori,[11] T. Rohaly,[10] A. Roodman,[3]
A. Sansoni,[5] R. D. Sard,[7] A. Savoy-Navarro,[4] V. Scarpine,[7] P. Schlabach,[7]
E. E. Schmidt,[4] M. H. Schub,[12] R. Schwitters,[6] A. Scribano,[11] S. Segler,[4]
Y. Seiya,[16] M. Sekiguchi,[16] P. Sestini,[11] M. Shapiro,[6] M. Sheaff,[18]
M. Shochet,[3] J. Siegrist,[9] P. Sinervo,[10] J. Skarha,[18] K. Sliwa,[17]
D. A. Smith,[11] F. D. Snider,[3] R. St. Denis,[6] A. Stefanini,[11]
R. L. Swartz, Jr.,[7] M. Takano,[16] K. Takikawa,[16] S. Tarem,[2] D. Theriot,[4]
M. Timko,[15] P. Tipton,[9] S. Tkaczyk,[4] A. Tollestrup,[4] G. Tonelli,[11]
J. Tonnison,[12] W. Trischuk,[6] Y. Tsay,[3] F. Ukegawa,[16] D. Underwood,[1]
R. Vidal,[4] R. G. Wagner,[1] R. L. Wagner,[4] J. Walsh,[10] T. Watts,[14]
R. Webb,[15] C. Wendt,[18] W. C. Wester, III,[9] T. Westhusing,[11]
S. N. White,[13] A. B. Wicklund,[1] H. H. Williams,[10] B. L. Winer,[9]
A. Yagil,[4] A. Yamashita,[16] K. Yasuoka,[16] G. P. Yeh,[4] J. Yoh,[4]
M. Yokoyama,[16] J. C. Yun,[4] F. Zetti[11]

[1] *Argonne National Laboratory, Argonne, Illinois 60439*

[2] *Brandeis University, Waltham, Massachusetts 02254*

[3] *University of Chicago, Chicago, Illinois 60637*

[4] *Fermi National Accelerator Laboratory, Batavia, Illinois 60510*

[5] *Laboratori Nazionali di Frascati, Istituto Nazionale di Fisica Nucleare, Frascati, Italy*

[6] *Harvard University, Cambridge, Massachusetts 02138*

[7] *University of Illinois, Urbana, Illinois 61801*

[8] *National Laboratory for High Energy Physics (KEK), Tsukuba, Ibaraki 305, Japan*

[9] *Lawrence Berkeley Laboratory, Berkeley, California 94720*

[10] *University of Pennsylvania, Philadelphia, Pennsylvania 19104*

[11] *Istituto Nazionale di Fisica Nucleare, University and Scuola Normale Superiore of Pisa, I-56100 Pisa, Italy*

[12] *Purdue University, West Lafayette, Indiana 47907*

[13] *Rockefeller University, New York, New York 10021*

[14] *Rutgers University, Piscataway, New Jersey 08854*

[15] *Texas A&M University, College Station, Texas 77843*

[16] *University of Tsukuba, Tsukuba, Ibaraki 305, Japan*

[17] *Tufts University, Medford, Massachusetts 02155*

[18] *University of Wisconsin, Madison, Wisconsin 53706*

[19] *Visitor*

1 Introduction

During the 1988/1989 run at the Fermilab Tevatron, the CDF detector collected $\simeq 4.1 pb^{-1}$ of $p\bar{p}$ data at $\sqrt{s} = 1.8$ TeV. The main goals of this run being physics at high p_t, the CDF trigger was "tuned" for maximizing signals from Z^0s, Ws, t-quarks, and *etc.* As such, compared to the high p_t physics, the b-physics program was of secondary importance other than that which would be used for background calculations. Also, CDF had no vertex chamber capability for seeing displaced vertices. However, significant b-quark physics results are evident in two data samples:

1. Inclusive electrons.
2. Inclusive J/ψ where $J/\psi \rightarrow \mu^+\mu^-$.

We can then ask ourselves, given all this, why is it that CDF is able to do b-quark physics? The answer is that nature has been kind enough to provide b-quarks at an extremely high rate at the Tevatron. The production cross-section for $b\bar{b}$ production is quite large, as table 1 implies.

Process	$\sigma_{produced}(\mu barns)$	Per inelastic
Unitarity ($\simeq 4\pi r^2_{proton}$)	120,000	
Inelastic ("minimum bias")	80,000	1/2
"QCD" (moderate→high Q^2)	1,000	1/50
$b\bar{b}$ X	40	1/1000
$W \rightarrow e\nu$	0.002	1/25,000,000
$t\bar{t}$ X ($m_{top} = 100GeV$)	0.0001	1/500,000,000

Table 1: A comparison of various "typical" production cross-sections at the Tevatron. All numbers are approximate.

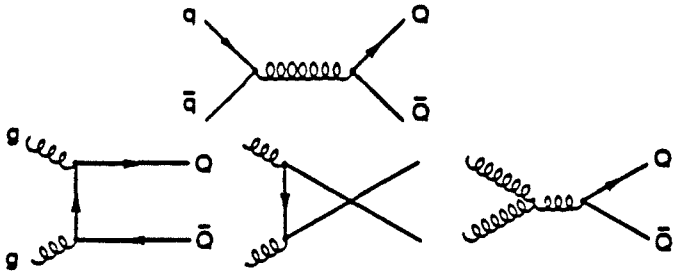

Figure 1. Lowest order graphs for $q\bar{q}$ production.

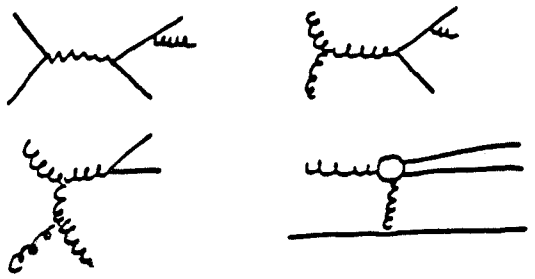

Figure 2. Next highest order graphs for $q\bar{q}$ production.

In the rest of this paper, I will try to specify the goals for b-physics using the inclusive electrons and J/ψ signals for the 1988/89 data set. I will then provide a brief look at the data, and will finish with some highly speculative guesses as to whether or not experiments at the Tevatron which look for CP violation in the b sector are possible.

2 B Physics Goals at CDF

There are many theoretical questions to answer concerning production properties of b quarks. For instance, due to the fact that the structure functions favor gluon interactions below $\sqrt{Q^2} \sim 30$ GeV (where the $b\bar{b}$ cross-section is highest), one expects that initial-state gg diagrams dominate over initial-state $q\bar{q}$ and qg. In figure 1 and 2 we show the lowest and next highest order diagrams, and of these the t-channel diagrams ("gluon fusion") dominate lowest order and the $gg \rightarrow gq\bar{q}$ ("gluon splitting") dominate at next highest order. Naively, the cross-section for the higher order amplitudes is expected to be of order α_s smaller than the tree level process due to the extra vertex. However, when the invariant mass of the $q\bar{q}$ is small compared to $\sqrt{\hat{s}}$, the energy of the subprocess, the process can be factored into a term for the production of gg (proportional to α_s) times the propagator $(1/m^2_{q\bar{q}})$ times the gluon splitting probability into $q\bar{q}$, or following Eichten[1]

$$\sigma(p\bar{p} \rightarrow q\bar{q}g) \simeq \sigma(p\bar{p} \rightarrow gg) \times \frac{\alpha_s}{2\pi} \int \frac{dm_{q\bar{q}}}{m_{q\bar{q}}} P_{g \rightarrow q\bar{q}}(x) dx.$$

and for production at pseudo-rapidity $\eta = 0$ in the CM frame

$$\sigma(p\bar{p} \rightarrow q\bar{q}g) = \sigma(p\bar{p} \rightarrow gg) \times \frac{\alpha_s}{3\pi} \ln(\frac{\hat{s}}{4m_q \bar{q}^2}).$$

Since the lowest order gg production cross-section is a factor of $\simeq 100$ times that for lowest order $q\bar{q}$, we see that $\sigma(p\bar{p} \rightarrow q\bar{q}g) \simeq \sigma(p\bar{p} \rightarrow q\bar{q})$. Note that these two processes (flavor creation *vs.* gluon splitting) may have different topologies and p_t dependencies, and as a source of backgrounds to high p_t processes such as $t\bar{t}$ production, it is crucial to measure the $b\bar{b}$ production

properties such as σ and $d\sigma/dp_t$. Predictions of $b\bar{b}$ production rates at the SSC would also be aided if the extrapolations (to small $x \equiv E/E_{beam}$ and large Q^2) started at 1.8 TeV from measured rates. For these reasons, the measurement of the $b\bar{b}$ production cross-section and $d\sigma/dp_t$ are some of the main goals of the CDF b-physics program.

Also, since the mixing for $B^0\overline{B^0}$ is large:

$$r \equiv \frac{\Gamma(B^0 \to \overline{B^0} \to \overline{X^0})}{\Gamma(B^0 \to X^0)} = 0.19 \pm 0.06 \pm 0.06[2]$$

a measurement of mixing using the like-sign electrons in the inclusive di-electron sample is another goal of the CDF b-physics program.

3 The CDF Detector

The CDF detector has been described in detail elsewhere [3]; here we describe relevant components in brief.

3.1 Tracking

Immediately outside the beam pipe are 8 time projection chambers (VTPC) providing $r - z$ tracking up to a radius of 22 cm in the pseudo-rapidity region $|\eta| < 3.5$. The primary use of the VTPC is in event vertex finding in z (with a resolution of $\delta z \simeq 1 - 2$ mm) and in identifying photon conversions in the VTPC/CTC (central tracking chamber) inner wall. Charge tracks are measured in a 1.412 Tesla axially field by the CTC, an axial drift chamber in the region $|\eta| < 1.2$. The chamber consists of 84 sense wires, 24 of which are tilted $\pm 3°$ to the axial direction for stereo determination. The wires are arranged in 9 superlayers, tilted for Lorentz angle compensation, extending to a radius of 1.3 m. Transverse momentum resolution $\delta p_t/p_t$ is measured to be $0.0017 p_t$ (Gev/c), and is improved to $0.0011 p_t$ using beam constrained fits.

3.2 Calorimetry

The CDF calorimetry consists of 3 subsystems in the regions $|\eta| \leq 1.1$ (central), $1.1 < |\eta| \leq 2.2$ (plug), and $2.2 < |\eta| \leq 4.2$ (forward). In this analysis, electrons are restricted to the central region and jets are restricted to the central and plug regions.

The central electromagnetic (CEM) calorimetry consists of alternating layers of lead with scintillator sampling, 18 radiation lengths deep, with projective tower geometry subtending $\delta\eta \times \delta\phi = .11 \times 15°$. The resolution measured using testbeam electrons between 10 and 50 GeV is found to be $\sigma/E = 13.5\%/\sqrt{E_t} \oplus 1.7\%$ where the two terms are added in quadrature and $E_t = E \sin\theta$ is in GeV. At shower max in the CEM ($6X_0$) are proportional wire chambers (CES) with cathode strip readout used to measure the azimuthal and axial position and shape of showers. The resolution measured using 25 GeV testbeam electrons is 2.0 mm in both the ϕ and z coordinates. Hadron showers are measured using iron-scintillator calorimeters (CHA and WHA) located radially behind the CEM. The resolution for testbeam pions is measured to be $\sigma/E \simeq 80\%/\sqrt{E}$. The phototubes are instrumented with TDCs which provide timing information used to reject cosmic ray and Main Ring backgrounds.

The plug and forward regions consist of gas proportional-tube calorimeters, both using lead absorber for EM showers and iron for hadronic and employing cathode pad readout. Projective towers cover $\delta\eta \times \delta\phi = .09 \times 5°$. The energy resolution for electrons and jets is measured to be $\sigma/E \simeq 30\%/\sqrt{E}$ and $\sigma/E \simeq 120\%/\sqrt{E}$ respectively.

3.3 Central Muons

Muons are identified in the central region $|\eta| < 0.65$ in drift chambers operated in streamer mode situated behind the 4.9 absorption lengths of the central EM and Hadron calorimeters. Chambers are segmented in ϕ into 12.6° wedges attached to the top of each calorimeter wedge, and there are 4 chambers per wedge. Single hit TDCs provide timing used to determine the ϕ coordinate in each chamber to $\delta r\phi \simeq 0.5$ mm. Charge division is

used to measure the z coordinate to $\delta z \simeq 5.0$ mm.

4 Inclusive Electrons

4.1 Trigger and Selection Criteria

For the 1988/89 Tevatron run, the inclusive electron trigger consisted of the following:

- Hardware levels:
  - Limited to the central tracking region $|\eta| \leq 1$
  - Hardware electron cluster defined by
    - ≤ 15 trigger towers ($\delta\eta = .2, \delta\phi = 15°$)
    - transverse electromagnetic (EM) energy $> E_t/1.125$ where E_t is the total transverse energy in the cluster
  - A match to a "stiff" CTC track in the same (ϕ) slice
  - 12 GeV trigger: EM $E_t \geq 12GeV$ and p_t of the track ≥ 5.5 GeV
  - 7 GeV trigger: EM $E_t \geq 7GeV$ and p_t of the track ≥ 4.8 GeV
- Software level:
  - Shower profiles in the strip chambers consistent with testbeam electrons.
  - E_t of the electrons above 12 GeV for the 12 GeV triggers and 7 GeV for the 7 GeV triggers

The efficiency for the 12 GeV trigger was studied using the missing transverse energy ($\not\!\!E_t$) triggers at "high" p_t and the $7GeV$ triggers at low p_t.

Offline, electrons in the central region are required to pass the following cuts:

- $\mathcal{L}_{shr} < 0.2$. This is a measure of how the lateral leakage of energy in an EM shower is consistent with testbeam data. The z vertex (from the VTPC) is used for this calculation.

- $\delta r\phi < 1.4$ cm and $\delta z < 2.0$ cm where $\delta r\phi$ and δz are the distances in $r\phi$ and z between a track as extrapolated from the CTC and the EM shower position as measured in the CES.

- $\overline{\chi^2} < 10$ where $\overline{\chi^2}$ is the average χ^2 of the shower profile (using testbeam electrons) in the $r\phi$ and z views in the CES.

- $Had/Em < 0.04$ in the cluster.

- 1 and only 1 charged track pointing to the cluster

- $0.75 < E/p < 1.40$ where E is measured from the cluster and p from the CTC.

Photon conversions are rejected searching for an oppositely charged track within $\delta(\cot\theta) < 0.06$ in the polar angle which has a distance of closest approach of less than 0.2 cm to the electron candidate. Candidate electrons which satisfy this cut and an additional criteria that for VTPC/CTC conversions there be less than 20% of the expected hits for a real electron in the appropriate road in the VTPC are removed.

After all cuts, we estimate the background to the prompt electron signal to be $15 \pm 15\%$ from charge hadrons and $12 \pm 7\%$ from residual photon conversions.

Additional backgrounds from $W \rightarrow e\nu$ and $Z \rightarrow e^+e^-$ decays are removed requiring the following:

1. $M_T^2 \equiv 2E_t\not{E}_t(1-\cos\delta\phi) > 64E_t$ where E_t is of the electron and $\not{E}_t$ is the length of the vector sum of the transverse energy in the calorimeters (with $|\eta| < 3.6$). This removes $W \rightarrow e\nu$ decays.

2. For all other clusters in the event which have EM fraction above 0.85 (EM cluster), we require the invariant mass of the electron candidate and the EM cluster $m(e, EM) > 80$ GeV. This removes $Z \rightarrow e^+e^-$ decays.

After all cuts, there are approximately 13,000 electrons from the $\simeq 225nb^{-1}$ of 7 GeV triggers and 17,000 from the $\simeq 4.1pb^{-1}$ of 12 GeV triggers. Figure 3 shows the p_t spectrum for these electrons before and after W/Z subtraction, and figure 4 shows the p_t spectrum for the conversion candidates.

4.2 Production Rates

The physics contribution to the inclusive electron distribution (not from backgrounds such as misidentification and conversions) are estimated using the ISAJET Monte Carlo. Event are produced from the following physics sources:

- $B_{d,u}$ mesons decaying semileptonically
- B_s mesons decaying semileptonically
- B baryons decaying semileptonically
- charm mesons decaying semileptonically
- cascade decays $b \rightarrow c \rightarrow l$
- $J/\psi \rightarrow l^+l^-$ production

After generation, all events were run through the full CDF detector simulation programs. The following table summarizes the results for electrons with $p_t > 12$ GeV.
The first row lists the fraction of the inclusive electron *produced* cross-section from the various sources. The second row lists the detection efficiency for each source. The last row contains the fraction of the *observed* inclusive electron cross-section from the various sources. We see that ISAJET predicts that 72% of the (real) inclusive electrons are from B-isospin mesons, and that 90% are from all B sources. Figure 5 shows the inclusive electron sample after W/Z removal with the ISAJET predictions for b and c to electrons superimposed (and a curve for c only) with arbitrary normalization.

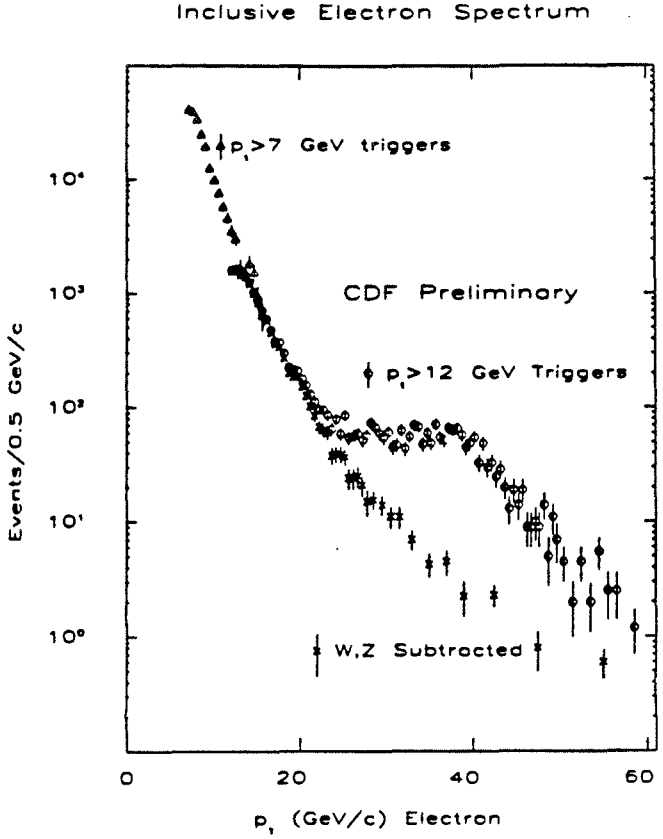

Figure 3. Inclusive lepton p_t spectrum.

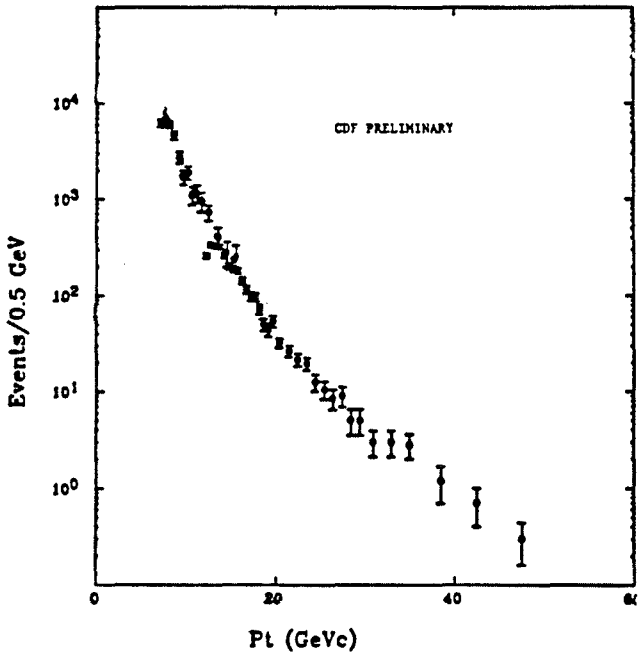

Figure 4. p_t spectrum for conversion candidates.

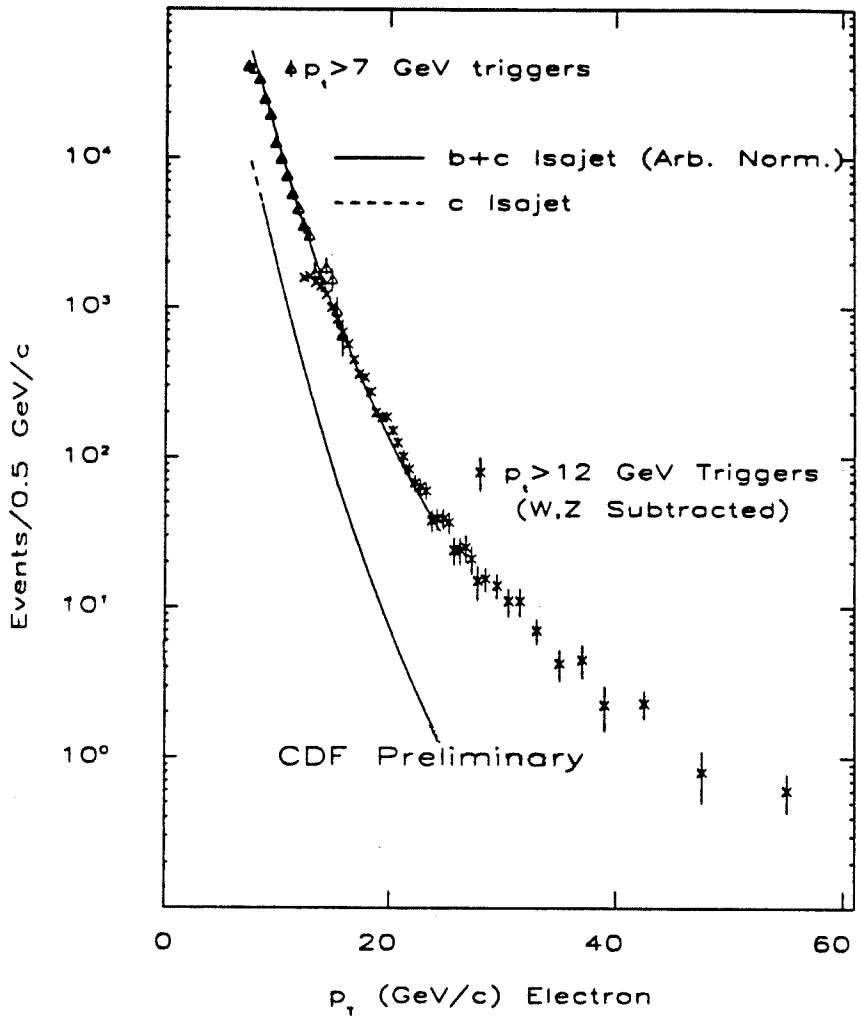

Figure 5. Inclusive lepton p_t spectrum: W/Z removed with leptons from ISAJET b and c quark decay.

	$B_{u,d}$	B_s	B_{baryon}	Charm	$b \rightarrow c \rightarrow e$	J/Ψ
Production Fraction	0.60	0.09	0.05	0.20	0.04	0.01
Detection Efficiency	0.43	0.43	0.35	0.17	0.13	0.55
Observed Fraction	0.72	0.12	0.05	0.09	0.01	0.01

Table 2: Fractions of electrons with $p_t > 12$ GeV from various sources.

4.3 $B \rightarrow D^0$

The above table predicts that 72% of the inclusive electrons in the region $|\eta| < 1, p_t > 12$ GeV are from $B_{u,d}$ mesons. Therefore, we search for evidence of D^0 mesons in these events via the decay $D^0 \rightarrow K^-\pi^+$ and $\overline{D}^0 \rightarrow K^+\pi^-$. To reduce backgrounds, we limit the the p_t of the electrons to be between 11 and 30 GeV. Note that the sign of the electron tags the charge state of the b quark and the sign of the kaon tags the charge state of the charm meson. The invariant mass of all pairs of oppositely charged tracks within a cone of $\Delta R = 0.6$ in $\eta\phi$ space ($\Delta R^2 \equiv \delta\eta^2 + \delta\phi^2$) around the electron are shown in figure 6. The momentum of the "kaon" track is then required to be above 1.5 GeV, and the sign is required to be the same as the electron (or positron). The peak above background contains $75 \pm 17(stat)$ events. ISAJET calculations predict 72 ± 20 events. Figure 7 shows a plot of the $K\pi e$ invariant mass for events in the region $|m(K\pi) - m_{D^0}| < 30$ MeV. The events in the sideband region defined by $30 < m(K\pi) - m_{D^0} < 90$

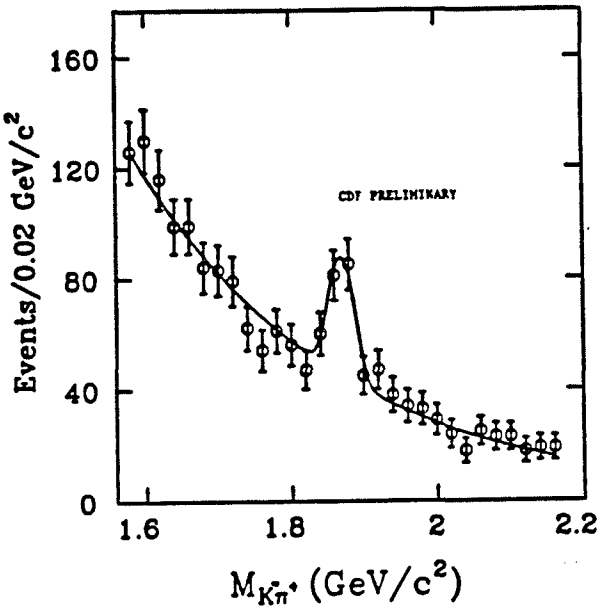

Figure 6. $K^{\pm}\pi^{\mp}$ invariant mass distribution ($p_t(K^{\pm}) > 1.5$ GeV, $\delta R(K\pi - \psi) < 0.6$).

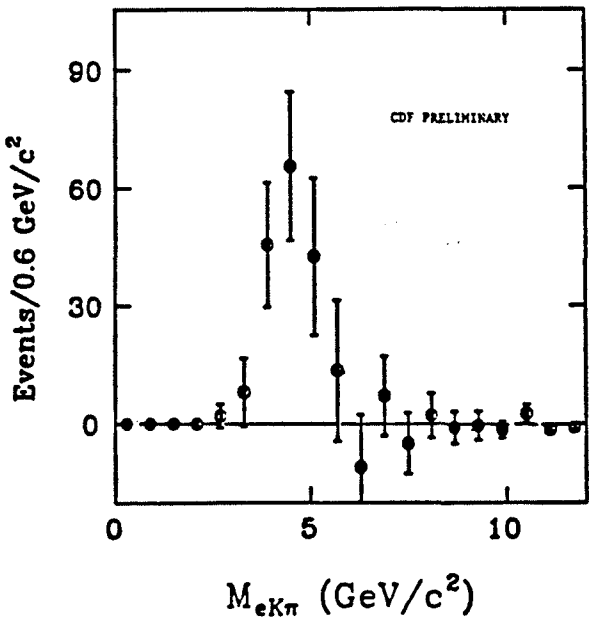

Figure 7. $K^{\pm}\pi^{\mp}e^{\pm}$ invariant mass with "wrong-sign-combination" $K\pi$ subtracted.

MeV and $-90 < m(K\pi) - m_{D^0} < -30$ MeV are subtracted, and for this plot the cone cut is opened up to $\Delta R < 1.2$. We see that within statistics the distribution falls to zero near the m_B threshold. This is as one would expect if the D^0s and electron were from a B meson decay.

Since b quarks are produced in pairs, one would expect to see D^0s produced in the "other" jet, which would result in kaons opposite in charge to the lepton, especially from for $b\bar{b}$ from flavor creation processes where the the lepton and D^0 will be on opposite sides of the detector (in $\eta\phi$ space). Figure 8 shows no evidence of a D^0 peak for events on the "other" side. This is under investigation, and may be due to at least one or more of the following reasons:

- $b\bar{b}$ quarks should be produced with some rapidity correlation such that $\delta\eta \sim 1$ or greater[4]. Also, one expects that the $b\bar{b}$ rapidity distribution to be rather flat out to rapidities of $\simeq 4$[4,5]. Since the tracking region of the CTC is limited to the region $|\eta| < 1$, this would cause a decrease in the acceptance for the "other" b given the detection of the first one.

- Qualitatively, a cut of $p_t^{electron} > 12$ GeV corresponds to roughly $p_t^b > 20$ GeV. This is far out on the tail of the b quark p_t distribution[6], where the efficiency for detecting $D^0 \rightarrow K^-\pi^+$ is expected to be reasonable. However, the b quark on the other side does not necessarily have the same high $p_t$as its partner, and hence will be more difficult to detect.

Work is continuing on this important question.

4.4 Inclusive Electrons - Goals and Speculation

At this date, a value for the mixing parameter (see section 2) is in progress. Also, since the semi-leptonic decay of the B_s meson should be $\simeq 100\%$ to the D_s meson ($B_s \rightarrow D_s e\nu X$), one might speculate that by looking for $D_s \rightarrow \phi\pi$ or $D_s \rightarrow K^{*0}K^+$ one may measure the mass of the B_s. This search is in progress. (However, as described below, CDF may have better measurements of these quantities using the inclusive $J/\psi \rightarrow \mu^+\mu^-$

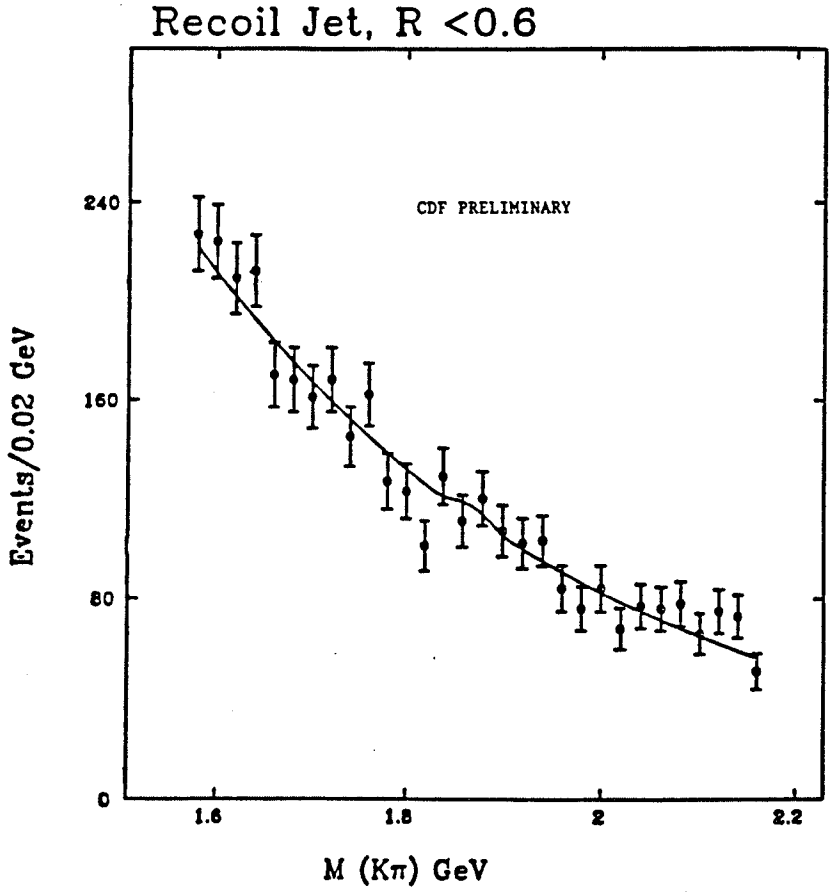

Figure 8. $K^{\pm}\pi^{\mp}$ invariant mass distribution in hemisphere opposite the electron candidate.

events). It is difficult to estimate how many events may be in the present sample due to many uncertainties, *e.g.* the fraction of B mesons which are B_s, the branching ratio of $b \rightarrow e$, and *etc.* "Reasonable" estimates put the produced number of events no larger than $\simeq 5$.

The next run is scheduled for mid-1991. CDF expects to record an increase in the luminosity of $\simeq \times 8$. With a lower trigger threshold, $12 \rightarrow 10$ GeV, an additional factor of $2-3$ may be gained. This would mean a sample of $\simeq 300,000$ inclusive leptons with $p_t > 10$ GeV on tape. CDF also plans to install a silicon vertex (SVX) chamber around the beam pipe to look for displaced vertices. With such a device and the expected amount of data, the B_s meson should be discovered and its lifetime and meson fraction $(B_s/B_{u,d})$ measured. This device will also help in studying lepton-D^0 events by required displaced vertices.

5 Exclusive Decays of B$\rightarrow \psi X$, $\psi \rightarrow \mu^+\mu^-$

5.1 Trigger and Selection Criteria

As mentioned above, the CDF central muon system covers the region $|\eta| < 0.6$ ($\cos\theta > 0.53$), and due to the construction of the chambers has an acceptance of $\simeq 83\% \times 2\pi$ in ϕ. The trigger consists of the following:

- Hardware Level 1: A central muon candidate is defined as having a coincidence between at least two out of four layers of the central muon chambers *with* roads defined to be 50% efficient for 3 GeV muons. See [3] for more details.
- Hardware Level 2: Requires 2 level 1 central muon candidates each having a track match in ϕ ($\pm 7.5°$) with $p_t > 3$ (90% efficiency point).
- Hardware Level 3: Requires the level 2 dimuon as above with an additional requirement that the two muons have $p_t > 3$ where here p_t is the momentum of the tracks matched in ϕ as determined by a fast, xy tracking reconstruction.

Offline, tracks are reconstructed using the full CDF tracking program, and "stubs" in the muon chambers are matched to tracks to form candidate muons with the requirement that $p_t > 3$. Due to hardware problems at the beginning of the run, only $\sim 3.0pb^{-1}$ of dimuon triggers were collected. Dimuon unlike-sign candidates are then used to search for J/ψ candidates. Figure 9 shows the invariant mass distribution of dimuon candidates where the p_t of the dimuon pair was required to be greater than 4 GeV. The distribution from like-sign dimuon pairs is also shown in this figure as a dashed line. There are approximately 1700 J/ψ events in the peak.

5.2 J/ψ Production

J/ψ particles are produced either directly as charmonium ($p\bar{p} \rightarrow c\bar{c}X$) or as decay products of other particles. Since the J/ψ has quantum numbers $J^{PC} = 1^{--}$, t-channel processes ($gg \rightarrow c\bar{c}$) which have 2 gluons in the initial state are suppressed relative to s-channel processes (*e.g.* $gg \rightarrow g \rightarrow c\bar{c}$) which have a single gluon in the initial state. However, in $p\bar{p}$ collisions for mass states as low as the J/ψ, t-channel processes dominate the production. This results in a suppression of *direct* J/ψ production relative to the production from decays, dominated by $\chi_{1,2} \rightarrow J/\psi\gamma$ and $B \rightarrow J/\psi X$. Again, since gluon fusion processes dominate, it is the mass state which determines the production rates at a given p_t. Therefore, one would expect that the process $\chi_{1,2} \rightarrow J/\psi\gamma$ will dominate at low p_t and $B \rightarrow J/\psi X$ dominate at a higher p_t (p_t of the J/ψ). Figure 10 shows the transverse momentum distribution of the J/ψ candidates along with a prediction from a calculation by Glover *et al.*[7]

5.3 $b\bar{b}$ Cross-section

There are many methods available for measuring the $b\bar{b}$ cross-section. At present, all results are preliminary. I will therefore describe some of the more promising methods which are being explored.

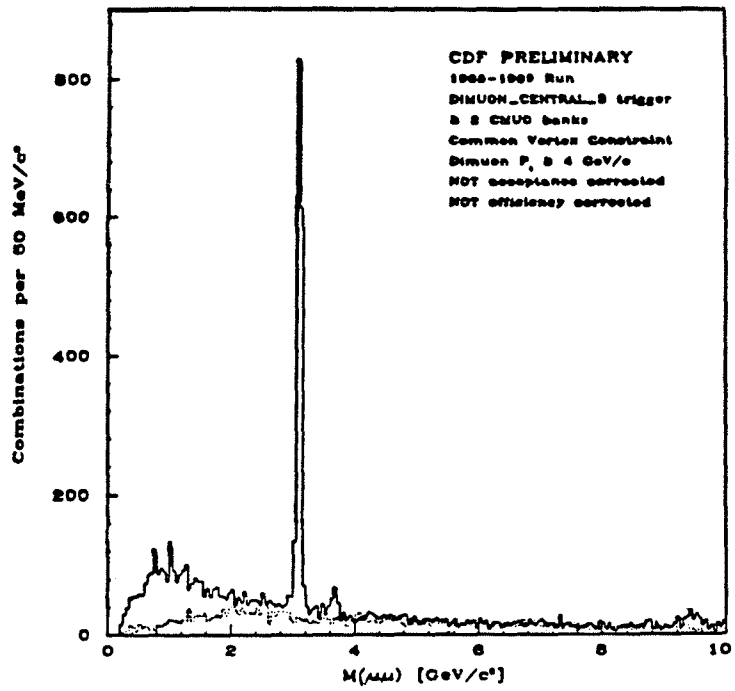

Figure 9. $\mu^+\mu^-$ invariant mass using dimuon triggers ($\mu^\pm\mu^\pm$ in dashes).

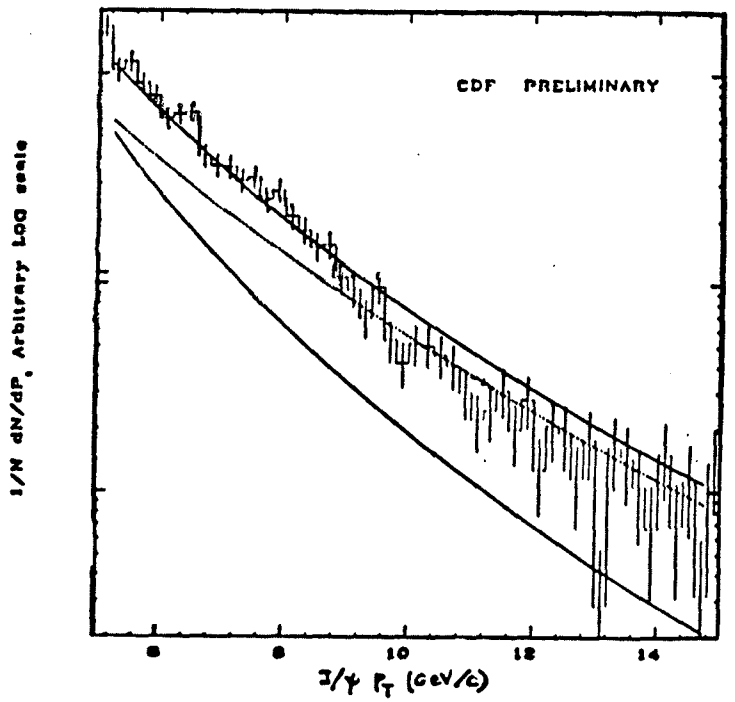

Figure 10. Dimuon p_t spectrum with Glover *etal.* calculation for J/ψ from $\chi_{1,2}$ (lower solid line), B decay (dotted line) and both (upper solid line).

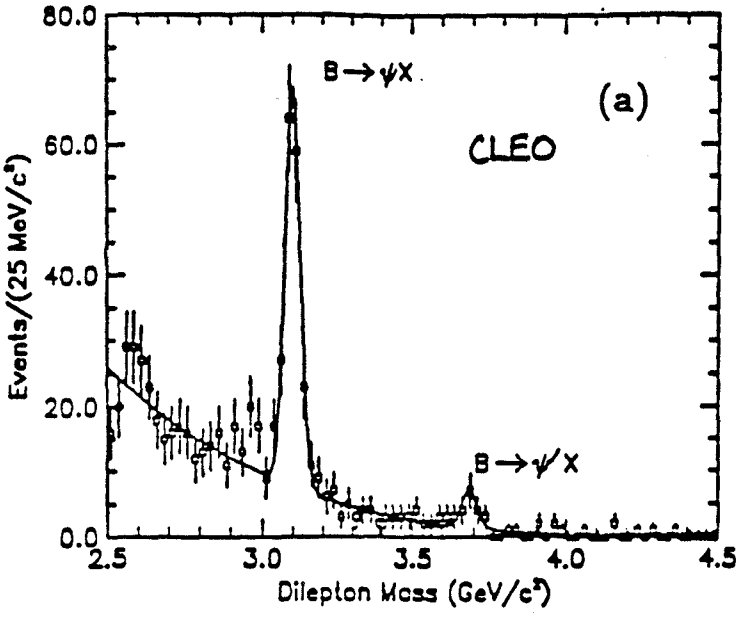

Figure 11. Dilepton mass from CLEO.

5.3.1 Event Topology

In producing J/ψ from $\chi_{1,2}$ decay, the p_t of the $\chi_{1,2}$ comes from recoil gluons, whereas lowest order $b\bar{b}$ can have nonzero p_t of the b-quark recoiling against a partner b. The event topologies are therefore expected to be different. For instance, J/ψ from B decay should be nearer to hadronic activity occurring in the same b-jet relative to $\chi_{1,2}$ where most of the remaining jet activity in the event is occurring in the recoil side. We therefore search for such a correlation in J/ψ-track and J/ψ-jet distributions. The analysis is at this time too preliminary to present here.

5.3.2 The Ratio $\sigma(\psi)/\sigma(\psi')$

Figure 11 shows the lepton invariant mass of dilepton pairs at the $\Upsilon(4S)$ as measured by the CLEO collaboration [8]. From figure 9, we see that the cross-section for detecting J/ψ' relative to J/ψ is quite a bit smaller at the Tevatron. Since theoretical prejudice has it that at the Tevatron $\simeq 100\%$ of all J/ψ' come from B decays, there must be another source of J/ψ production. By comparing with the CLEO result, one can extract the rate for $\chi_{1,2} \rightarrow \psi$, and use this to measure the $b\bar{b}$ production cross-section. This analysis is also in progress and will not be discussed here.

5.3.3 $\chi \rightarrow J/\psi\gamma$

The search for the decay $\chi_{1,2} \rightarrow J/\psi\gamma$ begins with the dimuon sample ($3.0pb^{-1}$). Muon candidate tracks are fit with a beam constraint. Figure 12 shows the dimuon invariant mass in the signal ($3.05 < m(\mu^+\mu^-) \leq 3.15$) and sideband ($2.80 < m(\mu^+\mu^-) \leq 3.00$ and $3.20 < m(\mu^+\mu^-) \leq 3.40$) regions.

For each muon candidate, the track extrapolation to the muon stubb is required to match within $\pm$5cm ($\simeq 2\sigma$) in the transverse plane. Photon candidates are restricted to central towers with $E_{EM} \geq 1.0$ GeV. The shower is required to be consisted with a photon shower in the CES (see above) by requiring $\chi^2_z, \chi^2_{r\phi} \leq 4$. The direction of the photon is calculated

from the position in the strip chamber and the event vertex as determined by the VTPC; the energy is tower EM energy. In order to reduce the combinatoric background from J/ψ decays from B mesons and to further the approximation that the energy of the photon is the sole contribution to the energy in the tower, we define an isolation variable using

- $\sum p_t$ of tracks (with $p_t > 1.0$ GeV) in a 30° cone and
- $\sum E \equiv \sum E_{HAD} + E_{EM}$ (with $E > 1.0$ GeV) in a 5×5 matrix of towers about the photon direction.

excluding the muons from the sums. The sum $\sum p_t + \sum E \leq 2.5$ GeV gives a background rejection of 70% with an efficiency of 80% using the ISAJET Monte Carlo and full CDF detector simulation.

After this cut, the mass difference $m(\mu^+\mu^-\gamma) - m(\mu^+\mu)$ is shown for the signal and side-band regions in figure 13, and a fit to the data using a gaussian signal over a background parameterized by

$$\sqrt{\Delta m} \cdot (a + b \cdot \Delta m + c \cdot (\Delta m)^2).$$

The fit yields 48 ± 15 events in the signal region centered at $\Delta m = 432 \pm 13$ MeV. The width is measured to be 74 ± 24 MeV. Calculations using the ISAJET Monte Carlo and full CDF simulation indicate that roughly 50% more J/ψ come from χ_1 than from χ_2. Using the values $m_{\chi_1} = 3.510$ GeV, $m_{\chi_2} = 3.556$ GeV, $m_\psi = 3.0969$ GeV, and the production fraction $\sigma(\chi_1) = 1.5 \cdot \sigma(\chi_2)$ we expect the mass difference to peak at 431 MeV, in good agreement with the data.

This analysis is still in progress, however it should yield a good measurement of the fraction of J/ψ decays from $\chi_{1,2}$ as a function of p_t, and thus a $b\bar{b}$ cross-section.

5.3.4 Exclusive Decays $B \to \psi K^+$ and $B \to \psi K^{*0}$

To look for exclusive decays of B mesons to J/ψ we use the entire $4.1 pb^{-1}$ dataset. Figure 14 shows a plot of J/ψ candidates (where there are $\simeq 2800$ candidates over a background of $\simeq 10\%$) and figure 15 shows a

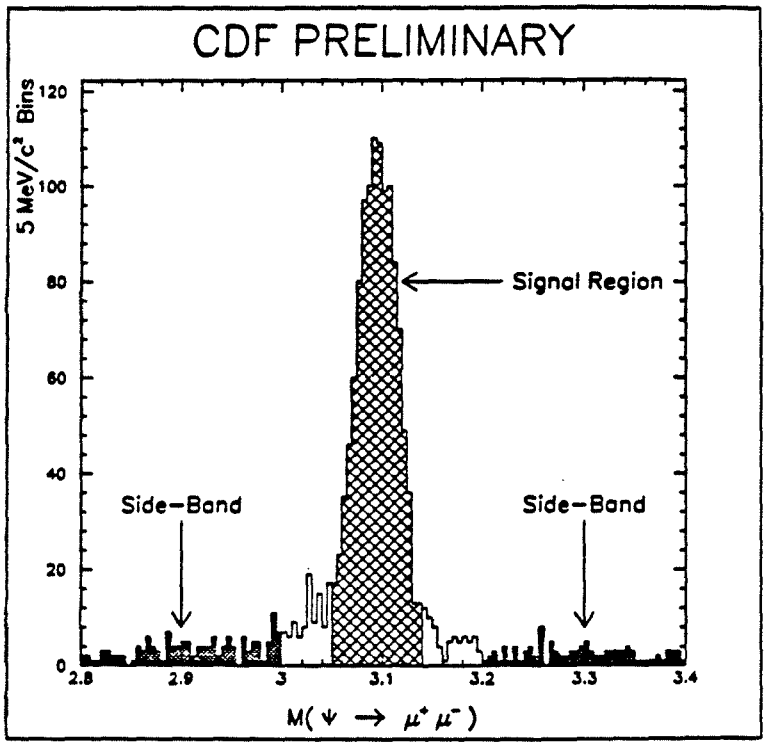

Figure 12. $\mu^+\mu^-$ invariant mass for χ sample.

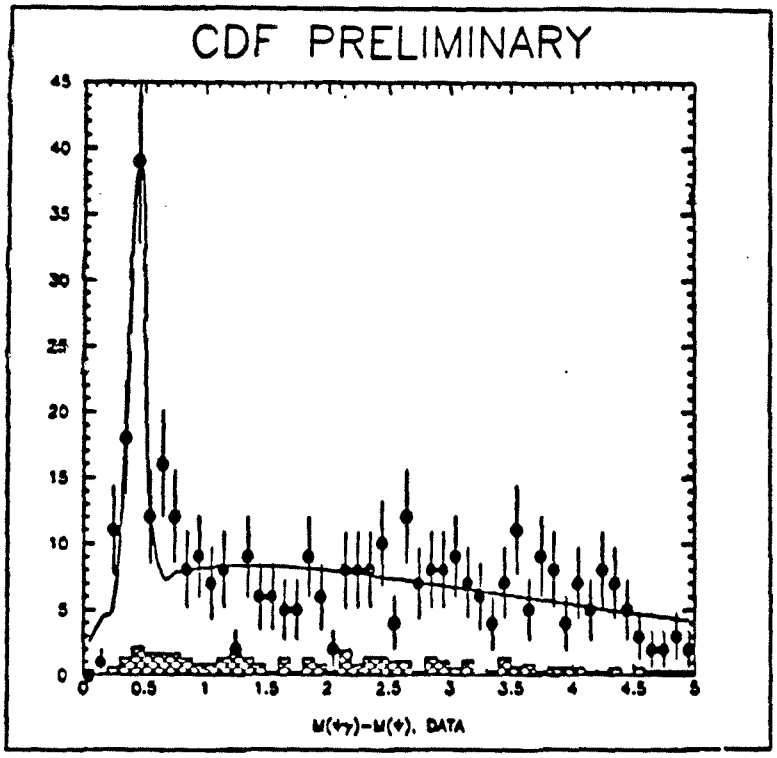

Figure 13. Distribution of $m(\mu^+\mu^-\gamma) - m(\mu^+\mu^-)$.

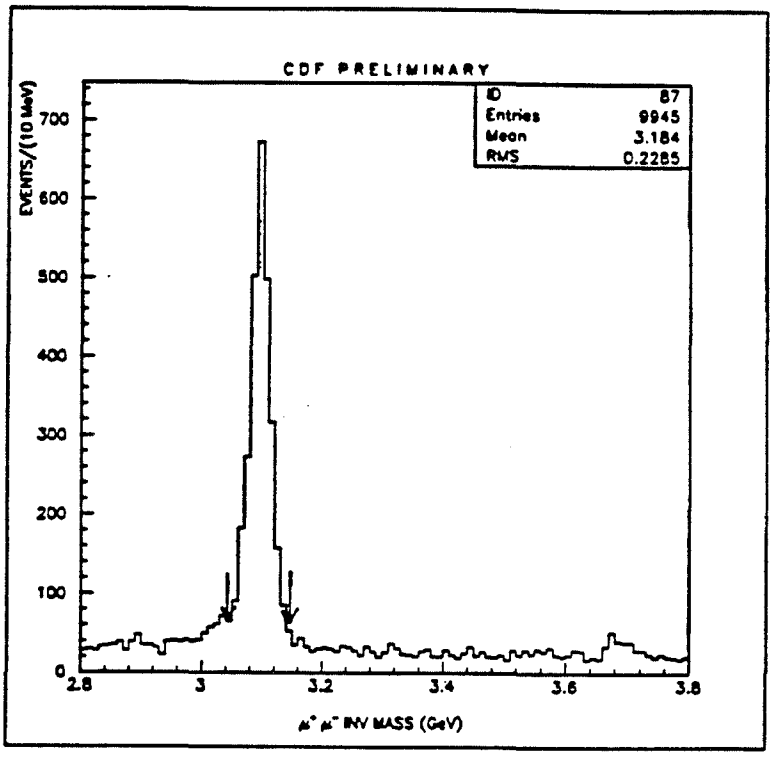

Figure 14. Full $4.1pb^{-1}$ dimuon sample.

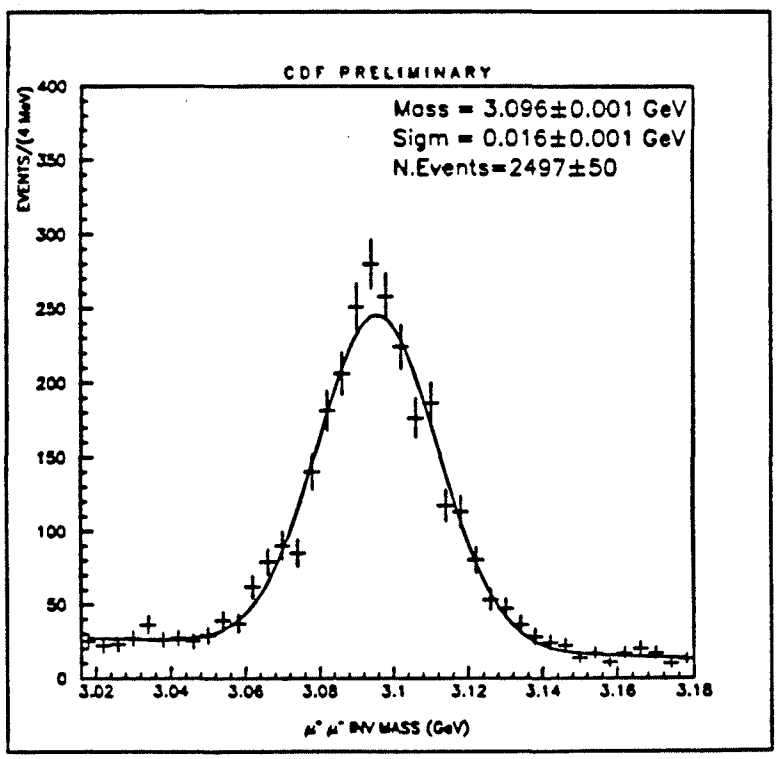

Figure 15. Fit to $\mu^+\mu^-$ in m_ψ region.

blowup of the distribution about the J/ψ mass, fit to a gaussian. The mean of figure 15 is consistent with the mass of the J/ψ to very high accuracy.

For exclusive decays, all dimuon pairs with $m(\mu^+\mu^-)$ in the signal region (defined by $|m(\mu^+\mu^-) - m_\psi| < 50$ MeV) refit with a mass constraint to $m_\psi = 3096.9$ MeV (the side-band regions are defined by $2.7 < m(\mu^+\mu^-) \leq 3.0$ and $3.2 < m(\mu^+\mu^-) \leq 3.5$). Charged tracks which are consistent with coming from the same event vertex in z as measured by the VTPC are then refit with a vertex constraint to that vertex. To reduce combinatorics, the following cuts are applied:

- Only tracks within a cone of 60° ($\Delta R \simeq 1$) about the J/ψ direction are used. This cut favors the high p_t B-mesons (relative to other sources of J/ψ production).
- The invariant mass of each J/ψ candidate and pairs of oppositely charged tracks ($m(J/\psi\pi^+\pi^-)$) are required to be more than 15 MeV away from the J/ψ' mass (see figure 16). Only tracks within a cone of 40° about the J/ψ are considered, and no momentum cuts are applied to these tracks.

All charged tracks with $p > 3$ GeV are assigned the K^- mass, and the invariant mass of these tracks and the J/ψ (mass constrained) candidates is shown in figure 17. An excess of $\simeq 20 \pm 6$ events at the B mass indicates the exclusive decay $B^\pm \to \psi K^\pm$. Figure 18 shows the same invariant mass distribution for J/ψ candidates in the above defined side-band regions. No excess appears at the B mass in this distribution.

In order to reduce the combinatorics in the search for $B^0 \to \psi K^{*0}$ where $K^{*0} \to K^+\pi^-$, only the three highest tracks in momentum are considered. Figure 19 shows the invariant mass of the 3 pairs of tracks where one is assigned the charged kaon mass. The natural width of the K^{*0} is $\simeq 50$ MeV. We therefore only consider pairs of tracks within ± 50 Mev of the K^{*0} mass, and form the invariant mass of the J/ψ candidate with these tracks. Figure 20 shows an excess of $\simeq 15 \pm 6$ events at the B mass. Figure 21 shows the invariant mass using the J/ψ candidates in the side-band regions, and figure 22 shows the invariant mass using the J/ψ candidates in the signal region and like-sign $K\pi$ pairs in the K^{*0} mass region. No excess at the B mass is seen in either of these two distributions.

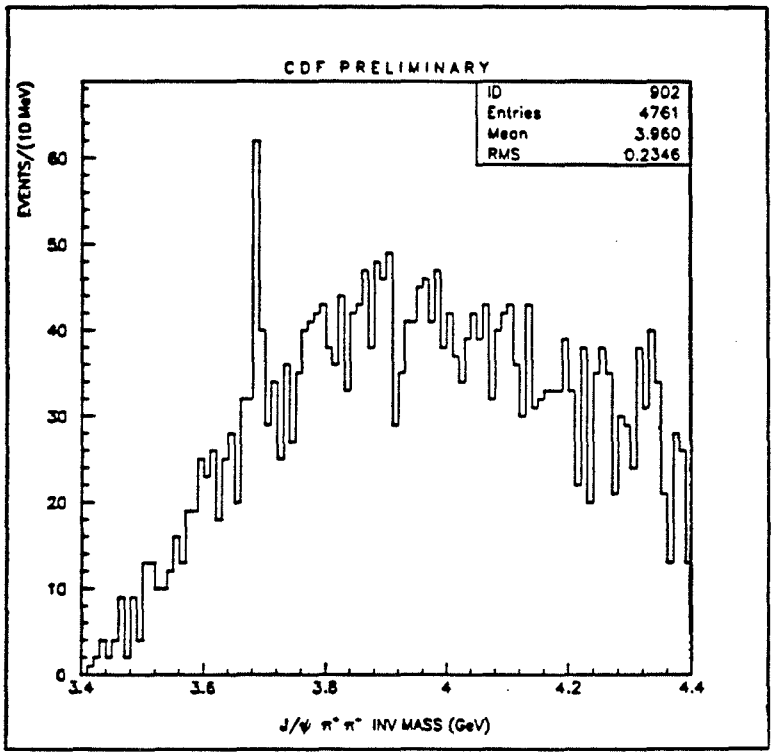

Figure 16. $J/\psi\pi^+\pi^-$ invariant mass distribution.

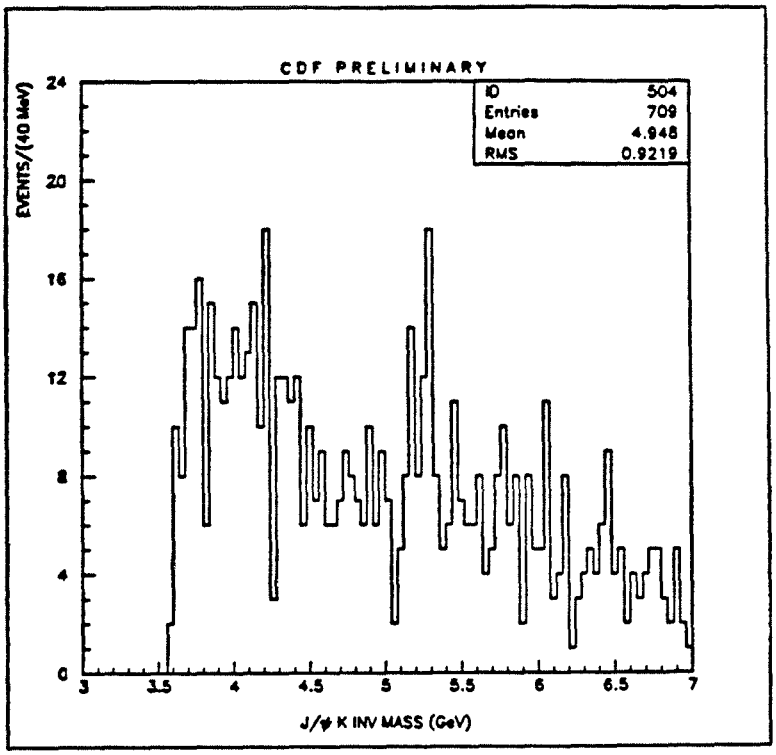

Figure 17. $J/\psi K^{\pm}$ invariant mass for $|m(\mu^+\mu^-) - m_\psi| < 50$ MeV.

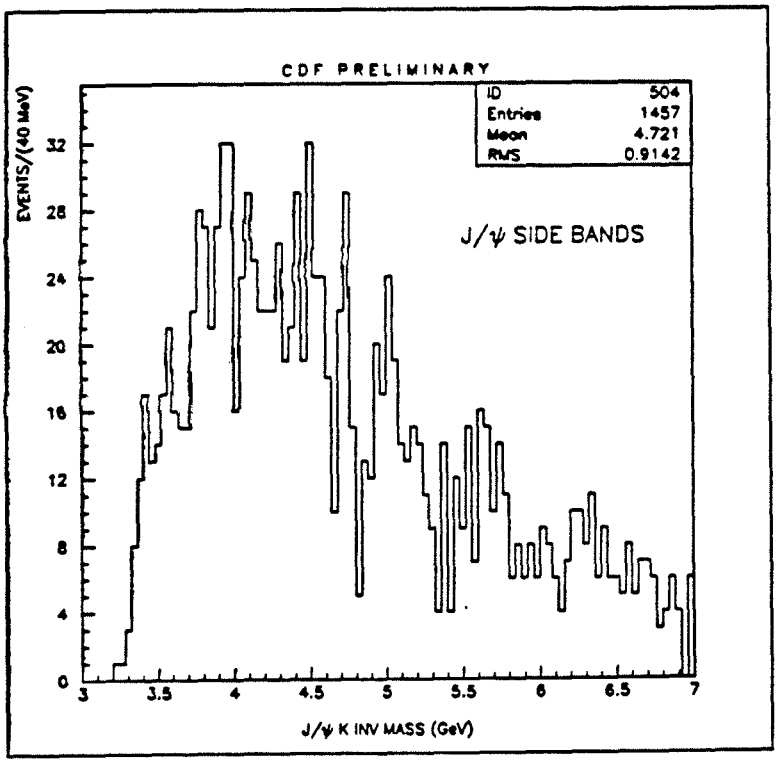

Figure 18. $J/\psi K^{\pm}$ invariant mass for $2.7 < m(\mu^+\mu^-) \leq 3.0$ and $3.2 < m(\mu^+\mu^-) \leq 3.5$

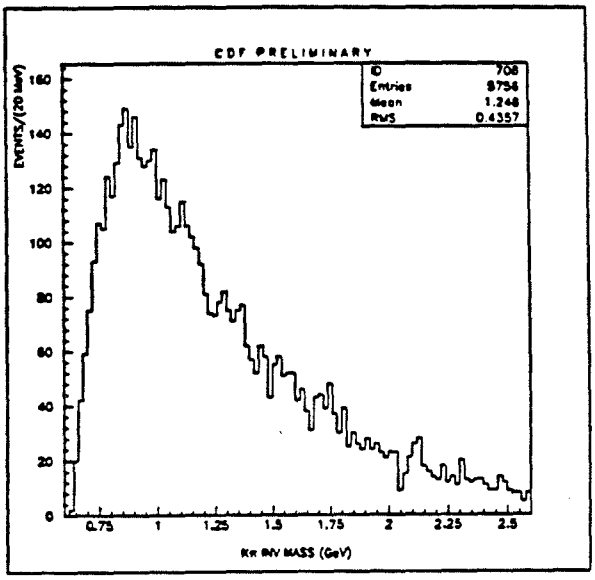

Figure 19. $K^{\pm}\pi^{\mp}$ invariant mass using only the highest 3 tracks in a cone 60° around the J/ψ direction.

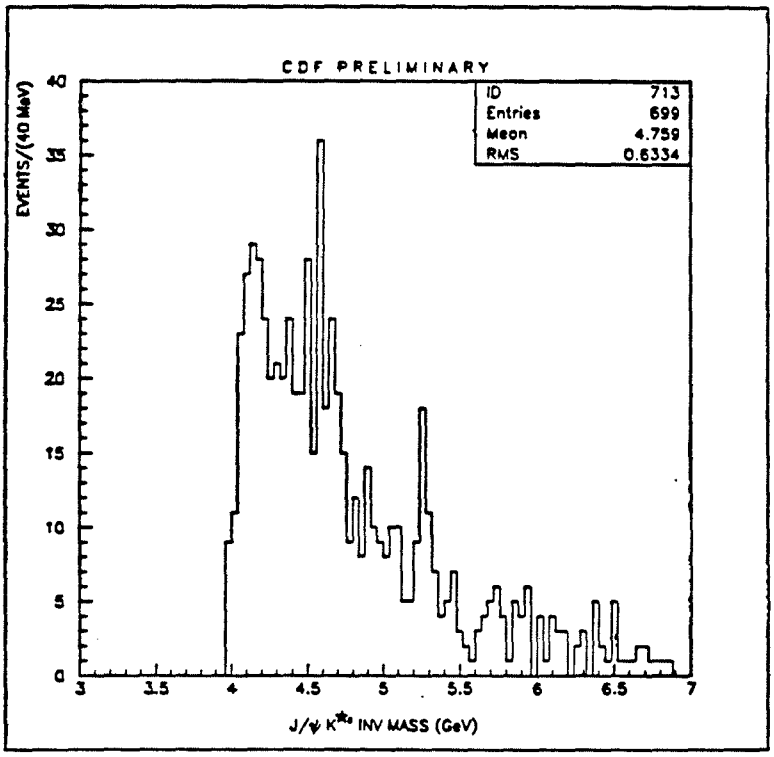

Figure 20. $J/\psi K^{\pm}\pi^{\mp}$ invariant mass with $|m(K^{\pm}\pi^{\mp}) - m_{K^{*0}}| < 50$ MeV.

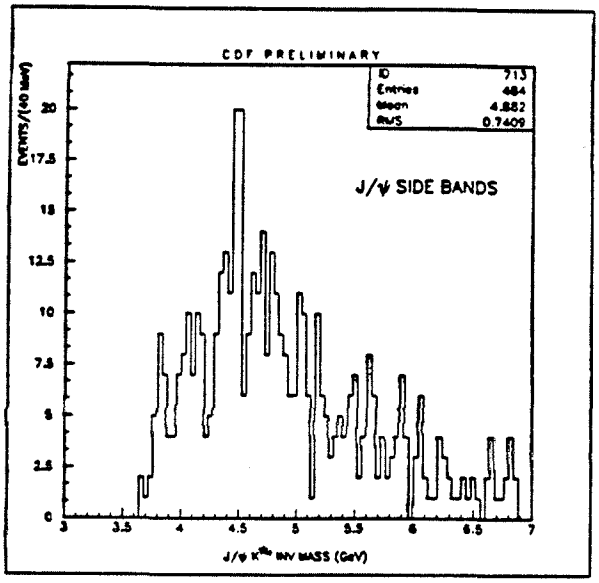

Figure 21. $J/\psi K^{\pm}\pi^{\mp}$ invariant mass with $2.7 < m(\mu^+\mu^-) \leq 3.0$ and $3.2 < m(\mu^+\mu^-) \leq 3.5$

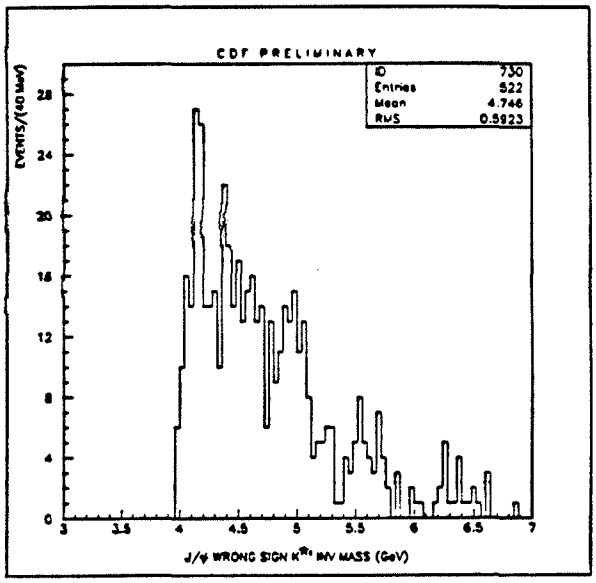

Figure 22. $J/\psi K^{\pm}\pi^{\pm}$ invariant mass.

Figure 23 shows the combination of the invariant mass distributions from figures 17 and 20. indicating an excess of $\simeq 35 \pm 9$ events at the $B_{u,d}$ mass.

6 CP Violation at the Tevatron

With the above promise for significant contributions by hadron colliders to B-physics, it might be worthwhile consider whether the ultimate goal of a B physics program, namely CP violation measurements, can be achieved. Just what one is going to measure at the Tevatron in order to see CP violation is discussed below.

6.1 Primer on CP Violation in the B sector

In any quantum mechanical process which can occur through more than one amplitude, interference phenomena can result in CP non-conservation. In the standard model of weak interactions the W boson interacts with mixtures of the quark mass eigenstates through the CKM matrix. The Hamiltonian for these interactions is given by

$$\mathcal{H} = \frac{g}{\sqrt{2}} W_\mu^+ \sum \overline{u}_i \gamma^\mu (1-\gamma_5) d_j V_{ij} + \frac{g}{\sqrt{2}} W_\mu^- \sum \overline{d}_j \gamma^\mu (1-\gamma_5) u_i V_{ij}^*$$

where u_i runs over u, c, t quarks and d_j runs over d, s, b quarks, g is an overall real coupling, and V_{ij} is the unitary CKM matrix. Under CP transformations, we have

$$(CP)\mathcal{H}(CP)^{-1} = \frac{g}{\sqrt{2}} W_\mu^- \sum \overline{d}_j \gamma^\mu (1-\gamma_5) u_i V_{ij} + \frac{g}{\sqrt{2}} W_\mu^+ \sum \overline{u}_i \gamma^\mu (1-\gamma_5) d_j V_{ij}^*$$

and we see that from comparing the above two equations, if V is real, then $\mathcal{H}$ is CP invariant. Although it is possible to absorb some of the complex phases of V into the quark fields u and d, Kobayashi and Maskawa

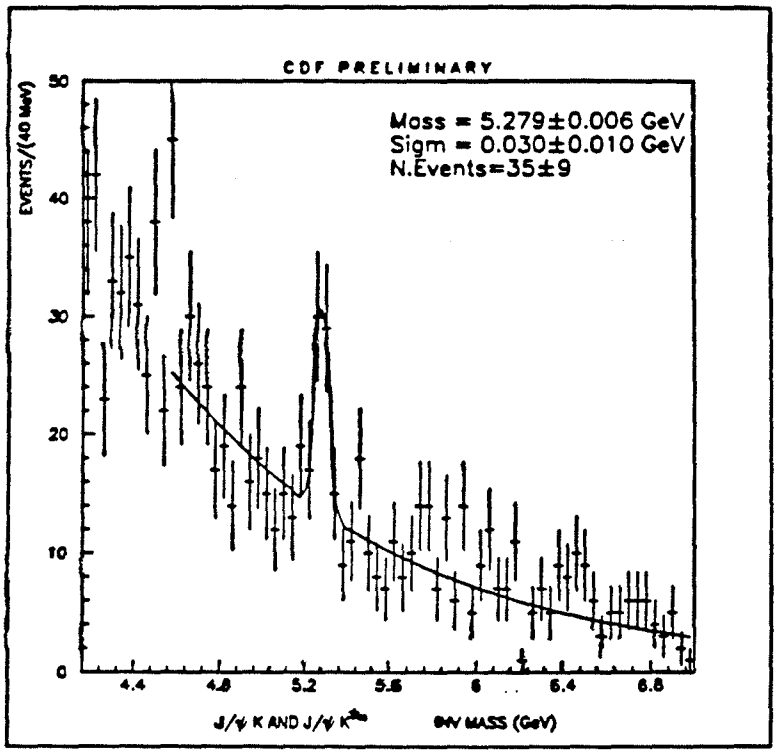

Figure 23. Combined $J/\psi K^{\pm}\pi^{\mp}$ and $J/\psi K^{\pm}$ invariant mass distributions.

[9] have shown that if V is a matrix 3×3 or larger, then V can contain complex phases which cannot all be absorbed by the fields. The weak interaction is therefore *in principle* capable of CP non-invariance provided the CKM matrix has at least one complex phase. One way that CP violation is expected to manifest itself is in the asymmetry in the decay rates of the B^0 *vs.* $\overline{B}^0$ mesons to CP eigenstates (*e.g.* ψK_s) through the interference in the $B^0/\overline{B}^0$ mixing amplitudes, or in plain english, $\Gamma(B^0 \rightarrow \overline{B}^0 \rightarrow X_{CP}) \neq \Gamma(\overline{B}^0 \rightarrow B^0 \rightarrow X_{CP})$ where X_{CP} is some CP-eigenstate decay product of both B^0 and $\overline{B}^0$. Another way to see this is to draw the lowest-order diagram for $B^0 \rightarrow \overline{B}^0$ mixing. If CP is violated, then T is violated (CPT is always conserved), the amplitude is different according to the time direction, and therefore not equal to the same diagram for $\overline{B}^0 \rightarrow B^0$.

We note that CP non-conservation can also come from final state interactions, but this will not be discussed here. In this paper, we will be referring to CP violation in the asymmetry in the decay of the neutral B mesons B^0 and $\overline{B}^0$ to the CP eigenstate ψK_s. Of course there are other ways for CP violation to manifest itself in the B-sector. We refer you to among other references a paper by Bigi and Sanda [10] and the recent **BCD** collaboration expression of interest (EOI) to the SSC laboratory which contains a comprehensive treatment of this subject.

Assume that one is going to look for an asymmetry in the rate for $B^0 \rightarrow \psi K_s$ using a lepton tag. The time evolution of the asymmetry (the difference divided by the sum) in the rates for B^0 *vs.* $\overline{B}^0$ to decay to ψK_s, is given by *Bigi et. al.*[10] (page 52, equation 2.13) and is:

$$A(t, \bar{t}, C = \pm) \propto \sin[(t \pm \bar{t})\delta m] \qquad (1)$$

where t and $\bar{t}$ are the proper times of the b and $\bar{b}$ systems respectively and δm is the mass difference between the mass eigenstates (B_1 and B_2 analogous to the kaon sectors) and the $\pm$ refers to the charge state (C) of the $b\bar{b}$.

First, let's look at CP violation at CESR. at the $\Upsilon(4S)$, where it is important to remember that $e^+e^- \rightarrow b\bar{b}$ proceeds via a virtual photon ($J^{PC} = 1^{--}$). Therefore the $b\bar{b}$ system is produced in a CP even (CP=+1) and C odd (C=-1) state, and equation 1 becomes

$$A(t, \bar{t}, C = -1) \propto \sin[(t - \bar{t})\delta m]$$

and the integral over both t and $\bar{t}$ from zero to infinity is equivalent to integrating the difference $\tau \equiv t - \bar{t}$ from $-\infty$ to ∞ over $\sin[\tau\delta m]d\tau$. This integral, being odd in τ, vanishes. Since at the Υ(4S) the $b\bar{b}$ system is in an odd charge parity (C=-1) state, we see that the asymmetry in the total rate vanishes, and therefore to see CP violation in lepton+ψK_s one has to actually measure the time asymmetry τ. However, at the Υ(4S) the b and $\bar{b}$ quarks are produced almost at rest, and so CP violation via measurements of τ are extremely difficult. In the C even case (C=+1) the integral does not vanish, CP violation can be manifested in the asymmetry, and it is therefore not necessary to measure the distribution in the proper times for the B^0 and $\overline{B}^0$ decays. In this case a counting measurement is sufficient, and one can integrate equation 1 to get a total asymmetry in the rate:

$$A = \frac{\Gamma(B^0\overline{B}^0 \rightarrow \psi K_s l^+) - \Gamma(B^0\overline{B}^0 \rightarrow \psi K_s l^-)}{\Gamma(B^0\overline{B}^0 \rightarrow \psi K_s l^+) + \Gamma(B^0\overline{B}^0 \rightarrow \psi K_s l^-)} \qquad (2)$$

where $l^{\pm}$ is from the lepton tag.

6.2 CP Violation at the Tevatron

At the Tevatron, the following characteristics are of note:

- The $b\bar{b}$ can be produced in either C=+1 or C=-1 states. Therefore one can simply measure an asymmetry in the rate (equation 2) as proposed above the $\Upsilon(4S)$ at CESR.
- Unlike in the e^+e^- experiments at or slightly above the Υ(4S) where B^0 mesons are produced almost entirely along with a $\overline{B}^0$, at the Tevatron, one expects neutral B mesons to be produced along with some combination of $\overline{B}^0$, B^*, $B^{\pm}$, B_s, and B_{baryon}. The asymmetry measurement is therefore the same as in equation 2 with no explicit requirement of having both B's neutral:

$$A = \frac{\Gamma(B\overline{B} \to \psi K_s l^+) - \Gamma(B\overline{B} \to \psi K_s l^-)}{\Gamma(B\overline{B} \to \psi K_s l^+) + \Gamma(B\overline{B} \to \psi K_s l^-)} \tag{3}$$

- The $b\bar{b}$ cross-section is huge. By "huge" we mean that relative to minimum bias, $\sigma(b\bar{b})/\sigma(mbs) \simeq 1/1000$.

Of course the important question asks how much luminosity CDF needs to see CP violation using the ψK_s events. To calculate this, we define

- N_B to be the number of $B \to \psi K_s$ observed in this year's data. The search for $B \to \psi K_s(K_s \to \pi^+\pi^-)$ is in progress, however we expect that there should be about $1/3$ as many of these events as $\psi K^\pm$ ($1/2$ from $K_s/K^\pm$ and $2/3$ from $Br(K_s \to \pi^+\pi^-)$, or $\simeq 6 \pm 2$ events.
- $\mathcal{L}_{\mu\mu}$ to be the luminosity for dimuon events ($\simeq 3/pb$)
- I_{91} to be the estimated increase in the dimuon rate ($\simeq \times 20$) due to the following three changes:
  1. trigger electronics changes should realize a factor of $\sim \times 3$ improvement in the *dimuon* trigger
  2. with the muon extension we get an increase of $\simeq \times 2$
  3. with a lower trigger threshold on p_t^μ in subsequent runs (lowered from ~ 3 to ~ 2) we can maybe get an additional factor of about $\simeq \times 4$ in the number of $\psi \to \mu^+\mu^-$.
- $Br_{B\to l}$ be the branching ratio of B to e or μ ($\simeq .1$)
- ϵ_l to be the efficiency for the lepton which includes the acceptance and p_t^l cuts

and calculate a detected cross-section for a tagged lepton (e/μ) and a $B \to \psi K_s$ to be

$$\sigma_{\psi K_s l^\pm} = \frac{N_B}{\mathcal{L}_{\mu\mu}} I_{91} 2Br(B \to l^\pm)\epsilon_l$$

(where the "2" is for e's and μ's). Plugging in the numbers we get

$$\sigma_{\psi K_s l^\pm} \simeq 2Br(B \rightarrow l^\pm)\epsilon_l \cdot 50pb$$

as the estimated detected cross-section. To calculate how much luminosity we need to see an N_σ effect in the asymmetry A (via equation 3) we use the fact that

$$\delta A = \sqrt{\frac{(1-A^2)}{N_{events}}}$$

and set $A/\delta A = N_\sigma$. Combining with the above cross-section we get:

$$\mathcal{L}_{CP} = \frac{N_{events}}{\sigma_{\psi K_s l^\pm}} = \frac{1}{50}\frac{N_\sigma^2(1-A^2)}{A^2}\frac{1}{2Br(B \rightarrow l^\pm)\epsilon_l}(pb^{-1}). \qquad (4)$$

If we use A=.16 and $N_\sigma = 3$, and tag both e and μ leptons with $Br(B \rightarrow l^\pm) = .1$ we get

$$\mathcal{L}_{CP} = \frac{0.035fb^{-1}}{\epsilon_l}$$

for the luminosity needed as a function of the lepton tagging efficiency. Note that the uncertainty in this number is quite large and is dominated by fluctuations in the presently observed number of $B \rightarrow \psi K_s$ events. It is conceivable that CDF will ultimately see $\sim 3fb^{-1}$ of luminosity in its lifetime, which means that the lepton tagging efficiency will have to be a few percent or more. Estimates from previous studies indicate that the fraction of *inclusive* Bs with a lepton above $p_t = 7GeV$ is about 1/100. However, since the luminosity required is proportional to $1/A^2$, any dilution of the asymmetry would make such an experiment very difficult. This is discussed in the next section.

6.3 Dilution of the CP-Violating Asymmetry

The above asymmetry will be diluted due to various physics (and detector) effects:

- The neutral B (B_s and B_d) which decays semileptonically can mix, hence will anti-tag the flavor state of the B which decays to ψK_s

- The CP state of the produced $b\bar{b}$ can be different from that of the final $B\overline{B}$ system. This can be the result of many different effects, for instance:
  - Either of the B mesons in the event can come from $B^* \rightarrow B\gamma$ decay. Events which had a single B^* will have an opposite C-parity for the $B\overline{B}$ relative to the producing $b\bar{b}$. Therefore, only events with C($b\bar{b}$) odd and one B^* or C($b\bar{b}$) even and either zero or two B^* will contribute to the asymmetry, since the integral over the proper times of the two mesons in the asymmetry (see equation 1) will vanish for odd C($B\overline{B}$)-parity states.
  - The $B\overline{B}$ can have relative angular momentum.
  - Final-state gluons can change the CP state - events with $B \rightarrow \psi K_s g$ where the g hadronizes.
- Background to the inclusive leptons used for tagging (fake leptons, leptons from charm, conversions, *etc.*) and from background ψK_s candidates.

In order to take into account all of these effects, detailed calculations are warranted. However, looking at equation 4, we see that $\mathcal{L}_{CP} \propto 1/A^2$ for small A. Any dilution of A of order 1/3 or larger will result in an increase in $\mathcal{L}_{CP}$ of an order of magnitude. We can therefore realistically conclude from this that CP violation at the Tevatron is probably *at least* more than 1 order of magnitude away from reality.

7 Conclusion

The future of B-physics at the Tevatron looks very bright. A high statistics ($\simeq 300,000$ inclusive leptons and $> 100,000$ $\psi \rightarrow \mu^+\mu^-$) sample of events for B-physics analysis using the CDF detector is a likely result of the coming (1991/92) run. The silicon vertex chamber will be installed, and with its $\simeq 10\mu$ resolution, displaced vertices from b decay should be reconstructible. It should therefore be possible for the CDF collaboration to measure

- With the inclusive lepton sample:
  - B_s mass, lifetime, and fraction
  - B^0 (and perhaps B_s) mixing
  - $b\bar{b}$ total and differential (with respect to p_t) cross-section with the relative contributions from flavor creation and gluon splitting amplitudes.
- With the inclusive J/ψ sample exploiting in particular the exclusive states $B \rightarrow \psi K^+$, $\psi K^{*0}(K^{*0} \rightarrow K^-\pi^+)$, $\psi K\pi^+\pi^-$, and $\psi K_s(K_s \rightarrow \pi^+\pi^-)$:
  - The $B^\pm$ and B^0 lifetimes
  - $b\bar{b}$ total and differential (with respect to p_t) cross-section with the relative contributions from flavor creation and gluon splitting amplitudes.

The dilution of the CP-violating asymmetry (as above) is sensitive to all of these quantities - their being measured would help determine whether CP violation is in principle a reasonable goal for the future.

References

[1] E. Eichten, Theoretical Expectations at Collider Energies, FERMILAB-Conf-85/178-T (1986).

[2] Artuso *et al.*, PRL. **62**, 2233 (1989).

[3] F. Abe *et al.*, CDF collaboration, Nucl. Instr. Method. **A271**, 387 (1988).

[4] R. K. Ellis, Fermilab-Conf-89/168-T (August, 1989).

[5] K. Foley *et al.*, Experiments, Detectors, and Experimental Areas for the Supercollider, edited by M.G.D. Gilchriese, World Scientific (1987), p. 701.

[6] P.Nason, S.Dawson, K.Ellis, Nucl. Phys. **B303**, 607 (1988).

[7] Glover, Martin, Stirling, Z.Phys. **38C**, 473 (1988).

[8] David Miller, Proceedings of the European Physical Society, Conference on High Energy Physics, Madrid 1989. "Recent Results from CLEO on B physics at the $\Upsilon(4S)$,

[9] M.Kobayashi,T.Maskawa, Prog. of Theo. Phys. **49**, 652 (1973).

[10] I.Bigi, A.Sanda, Nucl. Phys. **B281** (1987) 41.

[11] Artuso *et.al.*, PRL. **62**, 2233 (1989).

[12] P.Nason, S.Dawson, R.K.Ellis, Nucl.Phys. **B303**, 607 (1988).